Chapter 4
Optimization Results and Comparison

4.1 Introduction

The previous chapter introduced and classified the considered electromagnetic coupling architectures. Overall boundary conditions for centimeter scale vibration transducers were defined. In order to compare the performance limits of the architectures these boundary conditions are applied to all architectures. Then an optimization approach was formulated to assess the optimal dimensions with respect to the output power and the output voltage. For architectures with a 6–dimensional search space the evolution strategy optimization technique is used. Furthermore the architecture specific calculation of the magnetic flux gradient was discussed. The calculation of architectures without back iron is based on Maxwell's equations whereas the calculation of architectures with back iron is based on static magnetic 2–dimensional FEA.

Based on these assumptions this chapter discusses the results of the optimization and concludes with a comparison of the architectures' performance limits. This chapter is divided into four further subsections. In Sect. 4.2 the optimization results for the "Magnet in–line coil" architectures based on a cylindrical construction volume with a radius of 6 mm and a height of 8.90 mm (1 cm^3) are discussed. In the same manner, Sect. 4.3 considers the optimization results for the "Magnet across coil" architectures. For architecture A VI the cubic construction volume is defined as $10 \cdot 10 \cdot 10$ mm^3 and for the architectures A VII and A VIII $8.70 \cdot 8.70 \cdot 1.32$ mm^3 (in each case 1 cm^3). The reason for the different dimensions of the construction volume will be discussed in the subsections. Section 4.4 covers the comparison of the architectures' performance limit. Therein the advantages and disadvantages of each architecture are discussed and it is shown which architecture is best suited for maximum output power and maximum output voltage performance.

D. Spreemann and Y. Manoli, *Electromagnetic Vibration Energy Harvesting Devices*, Springer Series in Advanced Microelectronics 35, DOI 10.1007/978-94-007-2944-5_4,

4.2 "Magnet In–Line Coil" Architectures

4.2.1 Architecture A I

In A I a cylindrical magnet oscillates inside a cylindrical coil. The geometrical parameters are shown in Fig. 4.1. A special characteristic of this architecture is that the optimal resting position of the magnet is not directly apparent. It is plausible that when a magnet moves through the coil, the magnetic flux will increase until a maximum is reached and then decrease again. In between there is a point where the magnetic flux gradient has a maximum (exemplarily shown in Fig. 4.2). Because the magnetic flux gradient is directly proportional to the output voltage, this position defines the optimal resting position for output voltage maximization. However, due to the constrained construction volume condition the situation for maximum output power generation is different. This is because the power is dependent on both the voltage and the resistance of the coil. This results in a trade off and the first task for the optimization of A I is to find the optimal resting positions for both output power and output voltage generation, respectively.

The optimal resting position for arbitrary dimensions of the magnet in a fixed construction volume (defined by R_0 and h) can be obtained by varying the height of the coil and calculating the output power and output voltage (Fig. 4.3a). This was done for different magnet dimensions. The result shows that the optimal resting position is independent of the ratio of magnet and coil radii but depends on the ratio of their heights (Fig. 4.3b). Due to the dependence of the output power on the coil resistance, the optimal resting position for maximum power generation is shifted to lower values compared to the optimal resting position for maximum voltage generation. The least square polynomial curve fits of degree = 4 of the numerically determinded optimal resting positions are:

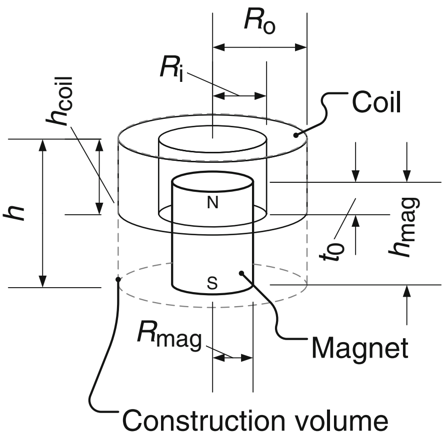

Fig. 4.1 Geometrical parameters of "Magnet in–line coil" architecture without back iron A I

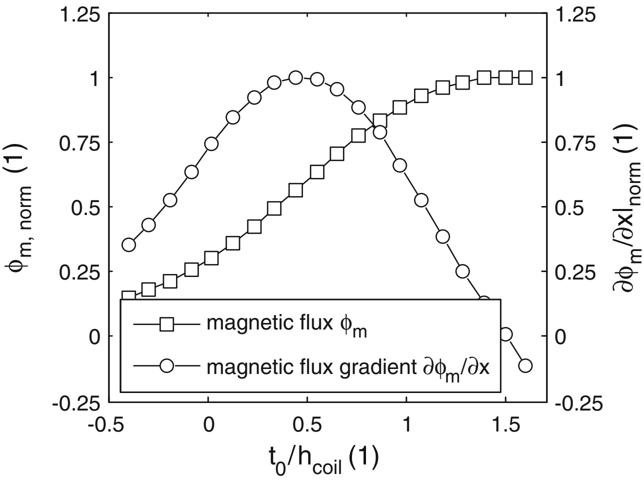

Fig. 4.2 When a magnet moves through a coil there is a point where the magnetic flux gradient is maximal. This point defines the optimal resting position of the magnet for output voltage generation but not for output power generation

Fig. 4.3 (**a**) To assess the optimal resting position in the fixed construction volume (defined by R_0 and h) the output power and output voltage has been calculated for different magnet dimensions and coil heights. (**b**) Resulting optimal resting positions for power– and voltage generation

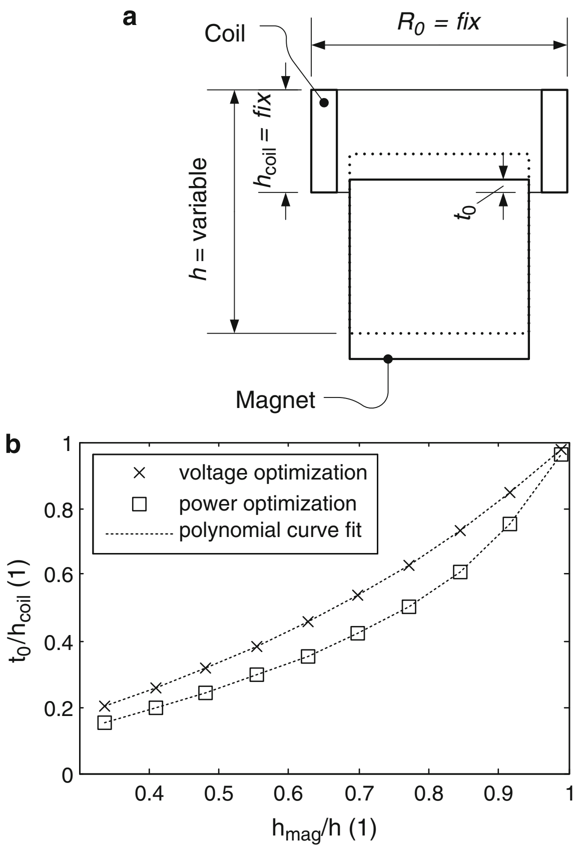

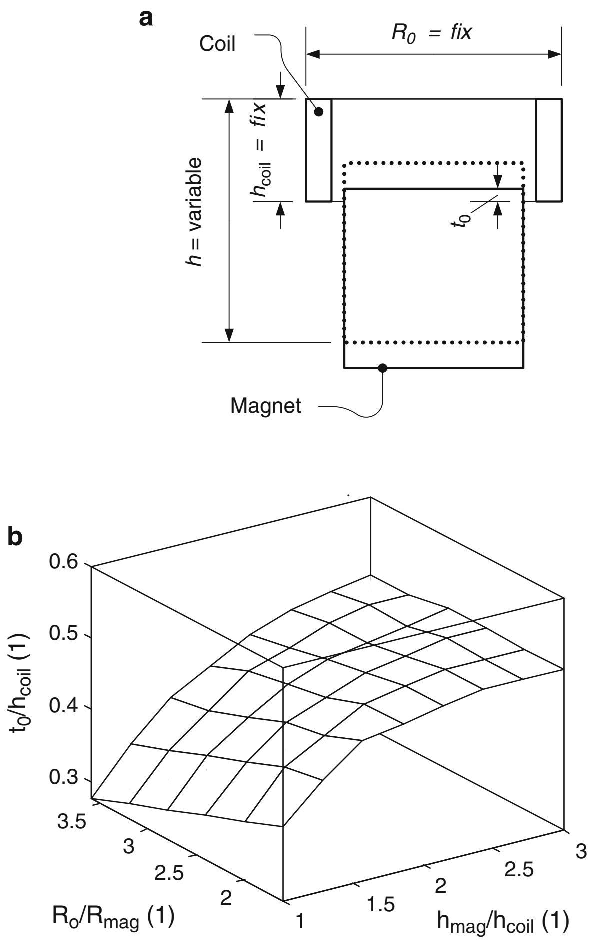

Fig. 4.4 (**a**) Variable construction volume condition has been applied in a previous publication to assess the optimal resting position [22]. (**b**) Resulting maximum magnetic flux gradient point for different ratios of coil to magnet height and radii

$$\frac{t_0}{h_{coil}} = 5.403\left(\frac{h_{mag}}{h}\right)^4 - 11.089\left(\frac{h_{mag}}{h}\right)^3 + 8.838\left(\frac{h_{mag}}{h}\right)^2 - 2.502\frac{h_{mag}}{h} + 0.348, \tag{4.1}$$

for output power generation and:

$$\frac{t_0}{h_{coil}} = 0.643\left(\frac{h_{mag}}{h}\right)^4 - 1.065\left(\frac{h_{mag}}{h}\right)^3 + 1.245\left(\frac{h_{mag}}{h}\right)^2 + 0.124\frac{h_{mag}}{h} + 0.052, \tag{4.2}$$

for output voltage generation. In a previous publication by the author of this book the optimal resting position has been calculated by varying the height of the construction volume as shown in Fig. 4.4a [22]. In this case the optimal resting position depends on the radii and the height of magnet and coil (Fig. 4.4b). However this approach is in contrast to the fixed construction volume condition considered in this book. Beyond this the maximum magnetic flux gradient point has been used as the resting position for the output power optimization. Hence the previous presented output power performance can further be increased using the optimal resting positions for output power generation.

Now that the optimal resting position has been defined the question to be answered is which height and inner radius of the coil yields a maximum power and voltage output? Note that due to the condition of fixed construction volume condition the height and radius of the magnet follows from the height and inner radius of the coil by using the optimal resting position and the gap size (defined by the boundary conditions). Hence there are two geometrical parameters to be optimized namely the inner radius and the height of the coil yielding a 2–dimensional search space. Using the optimal resting position for output power generation the optimization results with respect to the given boundary conditions are shown in Fig. 4.5. The resulting output parameters for different values of the coil radius and height are represented as contour plots. Starting with the inner displacement (Fig. 4.5a) it is evident that the higher the oscillating mass and the smaller the electromagnetic damping the higher the inner displacement. Hence, the highest inner displacement amplitude is obtained for the smallest winding area of the coil (h_{coil} small and R_{i} large). Because the oscillating mass depends on both the inner radius and the coil height, the isolines are somehow diagonal. Consequently, the coil's internal resistance increases with the coil winding area. In contrast to the inner displacement the highest resistances are obtained for large winding areas (h_{coil} large and R_{i} small) which is also valid for the optimal load resistance. Note that consistent with the EDAM, the values of the optimal load resistance (Fig. 4.5c) are greater than the internal resistance of the coil (Fig. 4.5b). Remember that this is due to the additional term of the parasitic damping electrical analog. Even more exciting is the result for the transduction factor (Fig. 4.5d), the output voltage (Fig. 4.5e) and the output power (Fig. 4.5f), where a maximum is inside the defined design domain (optimum marked with x, o and ▼, respectively). With respect to the transduction factor maximum the maximum for the output voltage is shifted to smaller coil heights and larger radii or in other words to higher oscillating amplitudes! This is plausible because the *emf* depends on both the transduction factor and the oscillating velocity. However, the goal at this point is not the optimization of the transduction factor or the output voltage but the output power. The optimum for the output power (Fig. 4.5f) is further shifted to higher oscillation amplitudes and smaller resistances with respect to the maximum of the output voltage. These results show that there are separate maxima for the transduction factor, the output voltage and the output power. The highest possible output power with respect to the given boundary conditions is 2.94 mW at 1.47 V for a coil with 5.41 mm inner radius and 2.53 mm height (53.5 mm^3 coil volume). The corresponding optimal ratio is $h_{\mathrm{mag}}/h = 0.92$ and $t_0/h_{\mathrm{coil}} = 0.75$ (Fig. 4.7a). Beyond these optimal dimensions the output power drops significantly which emphasizes the importance of optimized dimensioning. In general the output power of A I is rather sensitive to the coil inner

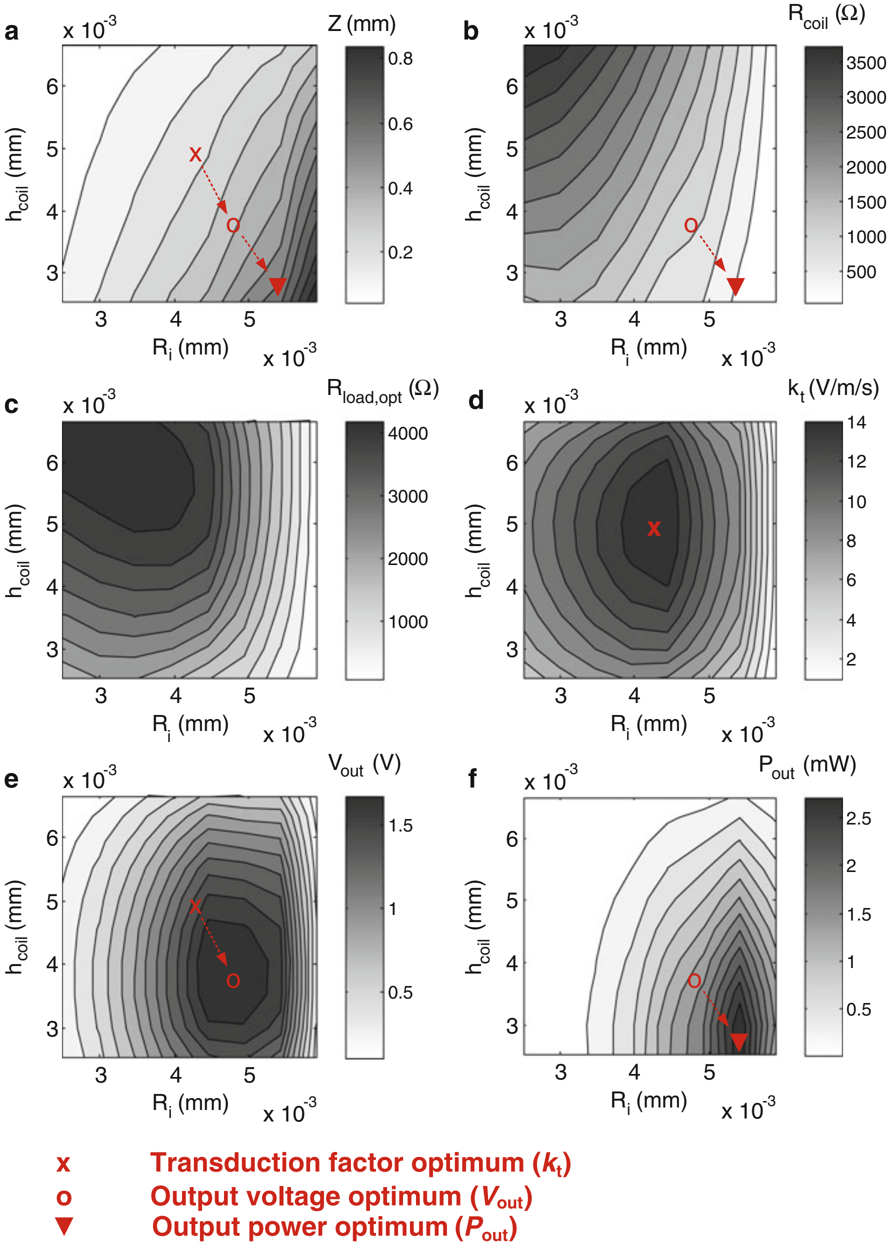

Fig. 4.5 Output power optimization result for A I in a construction volume of 1 cm³. The figures show the resulting (**a**) inner displacement amplitude, (**b**) coil resistance, (**c**) optimal load resistance for different dimensions of the coil. There are definitely different optimal dimensions for maximizing (**d**) the magnetic flux gradient, (**e**) the output voltage and (**f**) the output power

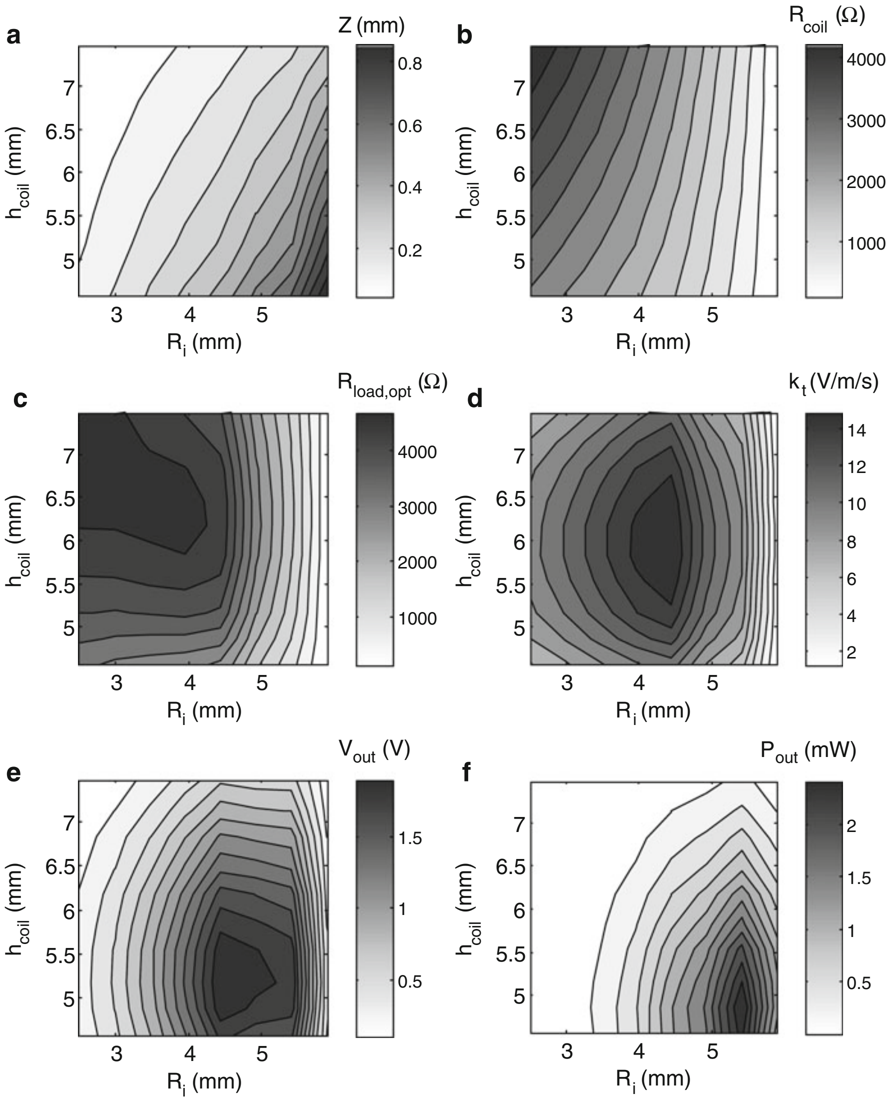

Fig. 4.6 Optimization result for A I in construction volume of 1 cm³ for operation at maximum magnetic flux gradient resting position (Voltage optimization). The arrangement of the figures is the same as in Fig. 4.5. Due to the different resting positions compared to the power optimization all the values are slightly higher apart from the output power which drops from 2.95 to 2.60 mW

radius as to the coil height. The result of output voltage optimization is shown in Fig. 4.6. In this case the optimal resting position for voltage generation has been applied. As previously explained, this point coincides with the maximum magnetic flux gradient point. Because this resting position comes along with a larger coil

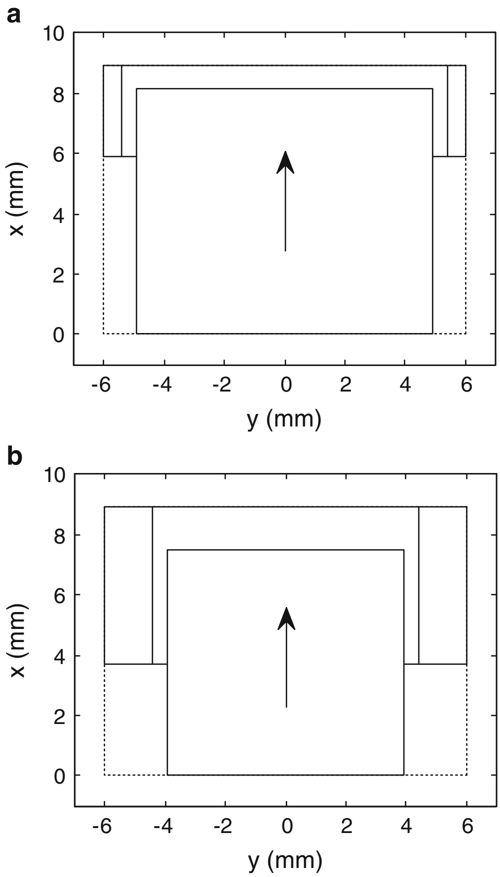

Fig. 4.7 Optimal dimensions for (**a**) output power and (**b**) output voltage generation with A I. The *arrows* point from north to south pole

winding area all the output parameters are slightly higher except the output power which drops slightly. The highest possible output voltage is 2.04 V at 1.08 mW for a coil with 4.44 mm inner radius and 5.14 mm height (263 mm³ coil volume). The corresponding optimal ratio is $h_{mag}/h = 0.84$ and $t_0/h_{coil} = 0.73$ (Fig. 4.7b). Thus the coil volume for power optimized dimensions is five times greater than the coil volume for voltage optimized dimensions.

4.2.2 Architecture A II

In A II a cylindrical magnet oscillates towards a cylindrical coil. In contrast to A I the magnet does not immerse into the coil. Hence the oscillation range of the magnet is limited and the resting position of the magnet is defined by the maximum inner displacement specified by the boundary conditions. The geometrical parameters are

Fig. 4.8 Geometrical parameters of "Magnet in-line coil" architecture without back iron A II

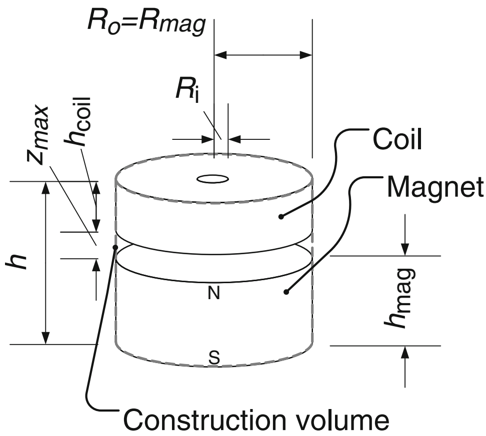

shown in Fig. 4.8. The geometrical parameters to be optimized are the inner radius and the height of the coil. The height of the magnet follows from the height of the coil:

$$h_{mag} = h - h_{coil}. \tag{4.3}$$

The results of the optimization in the cylindrical construction volume (again 6 mm radius and 8.9 mm height) are shown in Fig. 4.9. In A II the mass of the magnet depends on the height of the coil but not from the inner radius of the coil. Hence, the relative inner displacement amplitudes are almost horizontal isolines. However, for large inner radii the number of windings and hence also the electromagnetic coupling and the electromagnetic damping decreases. For this reason the inner displacement amplitude slightly increases. The optimum of the transduction factor and consequently also the optimum of the output voltage are limited to the minimum inner radius of the coil (set to $R_{i,min} = 0.5$ mm). Though, the output power is not limited to the inner radius even if the influence is barely observable. This is because the resistance of the inner windings are disproportional to their flux gradient. In the same way as for A I (refer to Fig. 4.5) the optimum of the transduction factor is shifted to higher inner displacement amplitudes with respect to the optimum of the output voltage. The optimum of the output voltage is in turn further shifted to higher oscillation amplitudes and smaller resistances concerning the optimum of the output power. The highest possible output power is 4.38 mW at 2.03 V for a coil with 2.50 mm inner radius and 0.82 mm height (76 mm^3 coil volume). The output voltage is maximized for a coil with 0.50 mm inner radius and 2.67 mm height (300 mm^3 coil volume). Therewith 3.59 V can be obtained at a power level of 2.87 mW. Note that the coil volume for voltage optimized dimensions is four times greater than the coil volume for power optimized dimensions. The optimal dimensions are shown in Fig. 4.10. In A II both the output power and the output voltage optimized dimensioning is more sensitive to the coil height than to the coil inner radius.

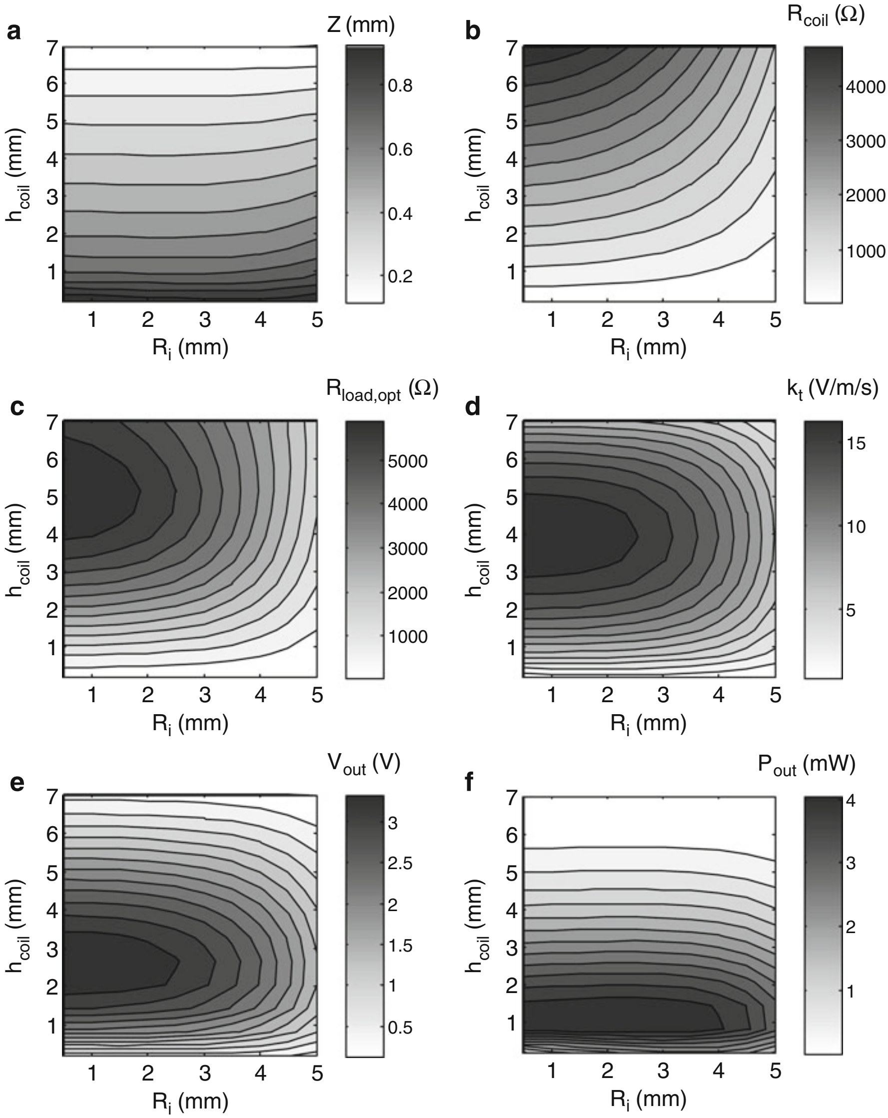

Fig. 4.9 Optimization result for A II in a construction volume of 1 cm³. The figures shows the resulting (**a**) inner displacement amplitude, (**b**) coil resistance, (**c**) optimal load resistance for different dimensions of the coil. There are definitely different optimal dimensions for maximizing (**d**) the magnetic flux gradient, (**e**) the output voltage and (**f**) the output power

4.2.3 Architecture A III

Architecture A III consists of two opposite polarized magnets which oscillate inside a coil. To reduce the repulsive forces between the magnets and to avoid

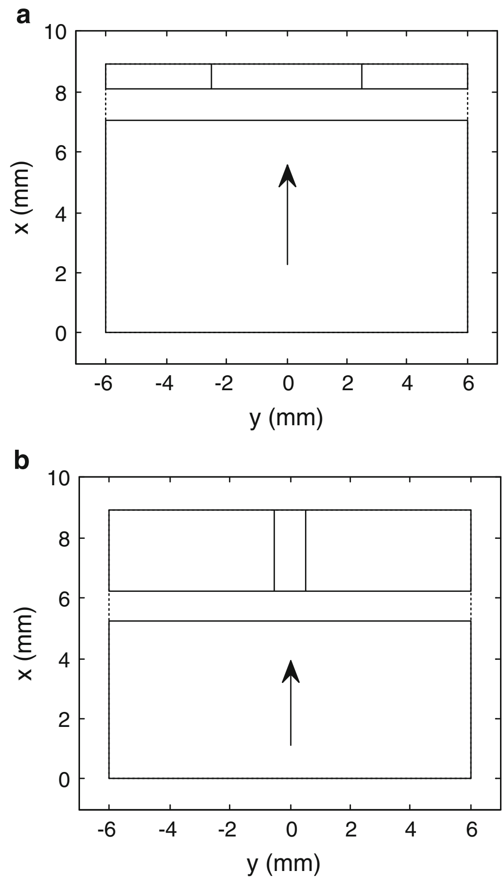

Fig. 4.10 Optimal dimensions for (**a**) output power and (**b**) output voltage generation with A II. The *arrows* point from north to south pole

demagnetization effects they are separated by a spacer. The geometrical parameters are shown in Fig. 4.11. In application the spacer is made of soft–magnetic material. To be able to compute the magnetic field distribution based on the semi–analytical magnetic field calculation approach the magnetic property of the spacer in the simulation is that of air. Note that this is a simplification because a soft magnetic material with high permeability will act as a flux connector and reduces the magnetic resistance. However as will be shown in (Sect. 5.2.3) the experimental verification of the simulation model shows that a ferromagnetic spacer has only a marginal influence and the results obtained with an “air” spacer are still accurate. The density of the spacer is equal to that of the back iron components defined by the boundary conditions. In the simulation a fixed height of the spacer $h_s = 2$ mm is used (in principle this dimension should be as small as possible but cannot be reduced arbitrary due to the repulsive forces). By doing so the parameters to be optimized are again the inner radius and the height of the coil. Due to the symmetry of the architecture the resting position is in the middle of the coil. Note that in the

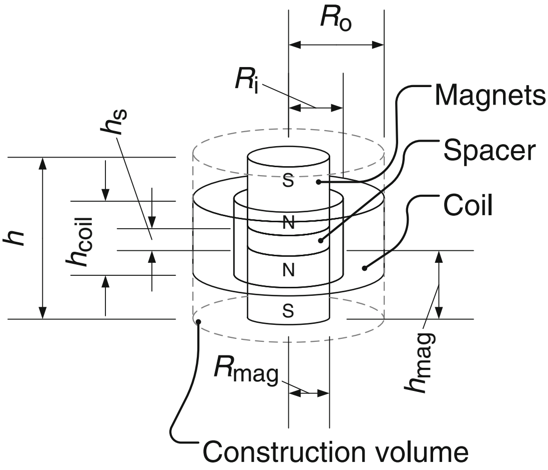

Fig. 4.11 Geometrical parameters of "Magnet in–line coil" architecture without back iron A III

simulation the magnetic flux gradient is calculated for only one magnet. Afterwards it is multiplied by two to obtain the overall magnetic flux gradient produced by both magnets.

The optimization results are shown in Fig. 4.12. In A III the mass of the magnet depends on the inner radius of the coil but not on the coil height. The relative inner displacement amplitudes are therefore almost vertical isolines. As for the previous architectures the maximum of the transduction factor is shifted to higher oscillation amplitudes concerning the output voltage and further to higher oscillation amplitudes and smaller internal resistances concerning the output power. The highest possible output power is 1.68 mW at 2.07 V for a coil with 5.34 mm inner radius and 4.93 mm height (37 mm^3 coil volume). The output voltage is maximized for a coil with 4.79 mm inner radius and 6.87 mm height (282 mm^3 coil volume). Therewith 2.64 V can be obtained at a power level of 1.06 mW. The optimal dimensions are shown in Fig. 4.13. The coil volume for voltage optimized dimensions is 7.6 times greater than the coil volume for power optimized dimensions. Beyond this the output power as well as the output voltage optimized dimensioning of A III is more sensitive to the coil inner radius than to the coil height.

4.2.4 Architecture A IV

A IV is the first architecture with a magnetic circuit based on back iron components. The geometrical parameters are shown in Fig. 4.14. The construction volume is defined by the outer radius R_o and the height h. In accordance to the previous convention all the components have to fit into the construction volume at the resting position of the oscillating mass. From there the coil is flush with the upper pole plate. However in practice the coil is required to protrude beyond the upper pole

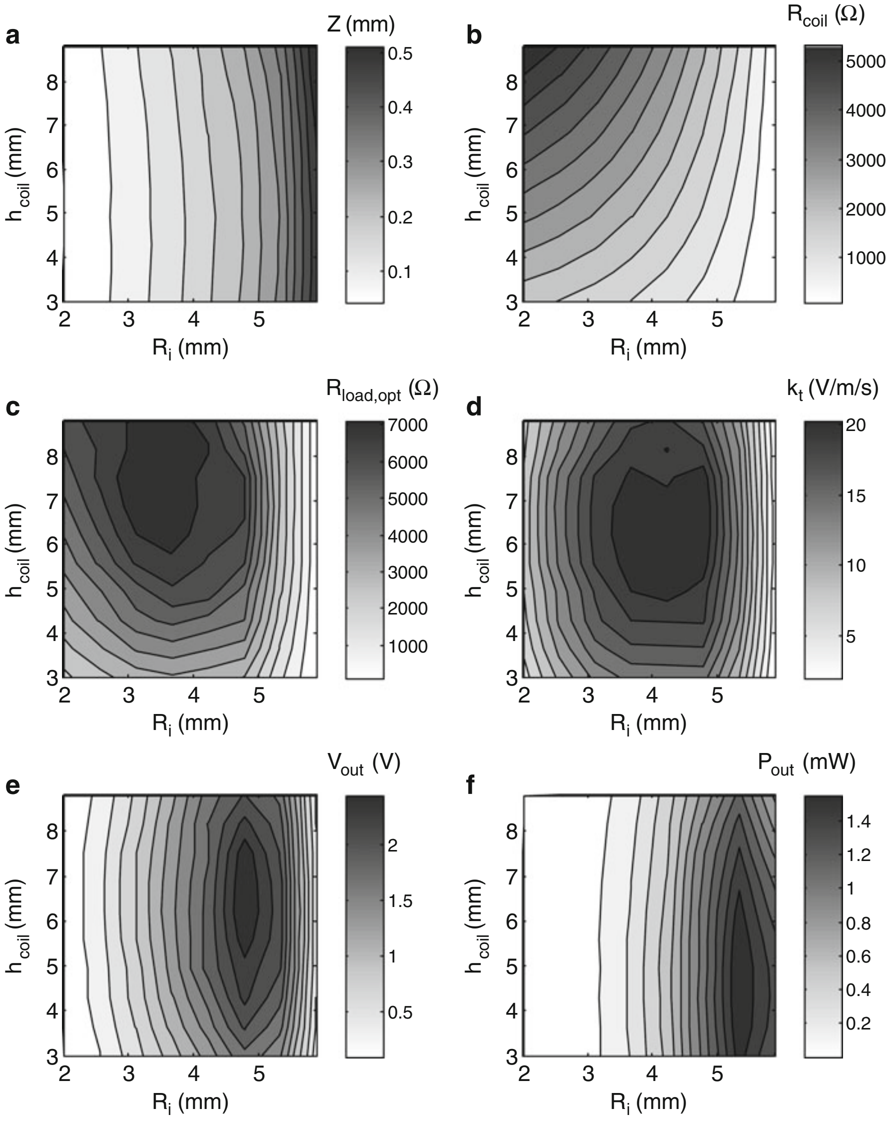

Fig. 4.12 Optimization result of A III in a construction volume of 1 cm³. The figures shows the resulting (**a**) inner displacement amplitude, (**b**) coil resistance, (**c**) optimal load resistance for different dimensions of the coil. There are definitely different optimal dimensions for maximizing (**d**) the magnetic flux gradient, (**e**) the output voltage and (**f**) the output power

plate, so that it can be fixed at a PCB or the housing. By looking at the geometrical parameters of A IV it is evident that, in contrast to the previous architectures, there are more than two independent geometrical parameters to be optimized.

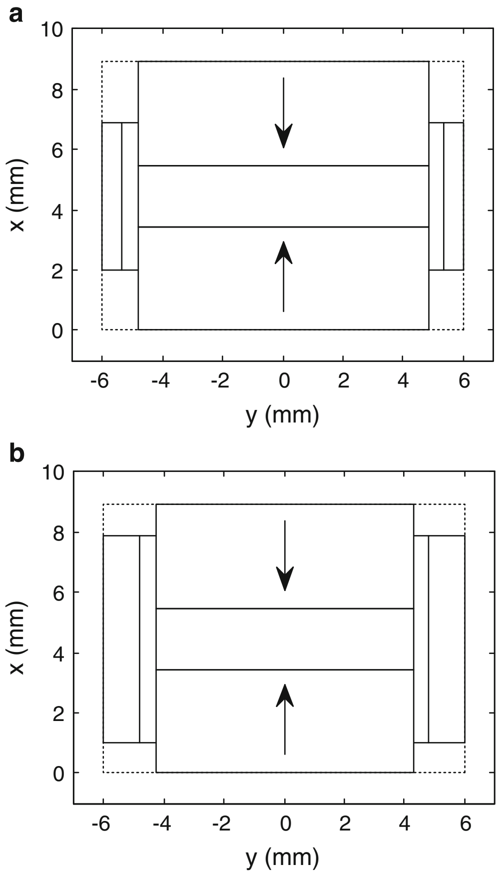

Fig. 4.13 Optimal dimensions for (**a**) output power and (**b**) output voltage generation with A III. The *arrows* point from north to south pole

These parameters are namely the height of the coil h_{coil}, the radius and height of the magnet R_{mag} and h_{mag}, the radius and the height of the upper pole plate R_{upp} and h_{upp} and the inner radius of the pot $R_{\text{i,pot}}$. These parameters lead to a 6–dimensional search space. In order to find optimal parameter sets for the output power and the output voltage generation the calculation procedure was integrated in an evolution strategy (ES) optimization technique (as discussed in Sect. 3.5.2). Figure 4.15a shows the convergence of an output power ES optimization run where the mean value of the fitness (output power) of the selected individuals is plotted versus the number of generations. After 80 generations the optimization converges and there is no significant increase of the fitness of further generations. At this point the selected individuals are very similar and the best individual of the optimization run (taken from generation 78) can be assumed to be an optimal parameter set. Figure 4.15b is a plot of the corresponding success rate and the standard deviation. Because the success rate after the 3rd generation is already below 1/5 the standard deviation steadily decreases from the maximum of 0.08 to the minimum of 0.005. In the same

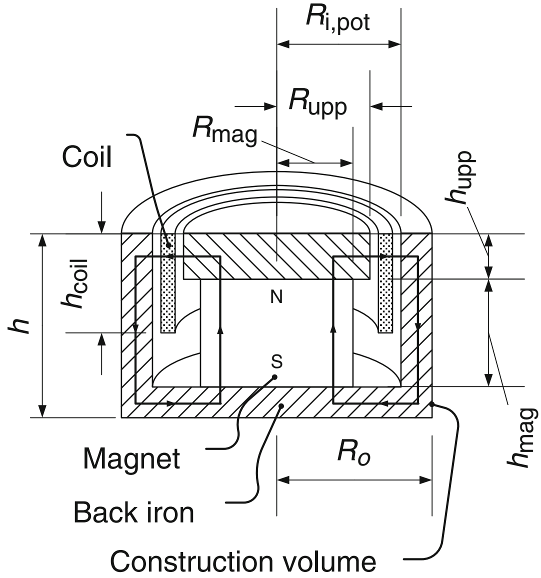

Fig. 4.14 Geometrical parameters of "Magnet in–line coil" architecture with back iron A IV. The *closed loop* indicates the direction of magnetic flux

manner Fig. 4.15c, d shows the result for an output voltage ES optimization run. Here the algorithm converges already after 30 generations. The best individual is within generation 23. The magnetic field pattern for output power and output voltage optimized dimensions of A IV is shown in Fig. 4.16a, b. With these optimized dimensions a maximum output power of 5.81 mW can be generated at a voltage level of 1.73 V and a maximum output voltage of 3.14 V at a power level of 3.25 mW. The coil volume of the output power optimized design (37 mm^3) is more than five times smaller than the volume of the output voltage optimized design (195 mm^3). Note that due to the effect of field homogenisation and concentration it is advantageous in moving coil loudspeakers to make the radius of the magnet smaller than the radius of the upper pole plate ($R_{mag} < R_{upp}$) [1]. However in vibration transducers this advantage cannot compensate the disadvantage of the lost mass. That's why the radius of the magnet should always be equal to the radius of the pole plate.

4.2.5 Architecture A V

Architecture A V is similar to A IV. However in A V a ring magnet is used instead of a cylindrical magnet. The geometrical parameters are shown in Fig. 4.17. Again, the number of independent geometrical parameters for the optimization led to a 6–dimensional search space and ES optimization is applied to find optimal parameter sets. The parameters are namely the height of the coil h_{coil}, the inner

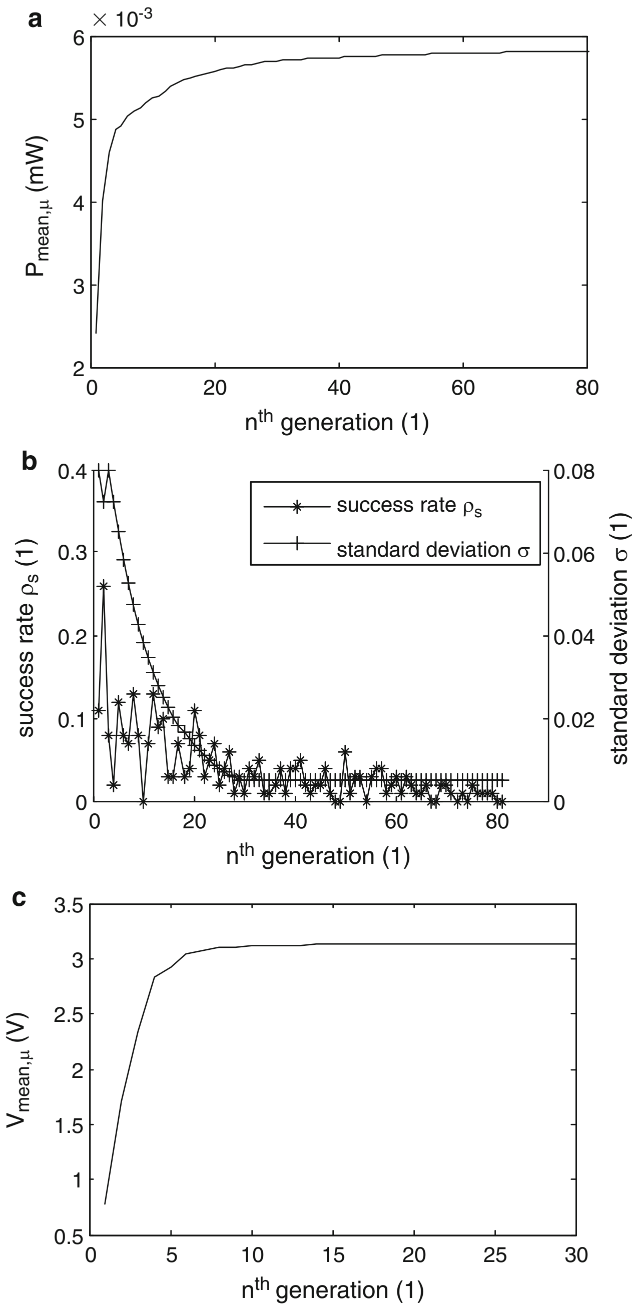

Fig. 4.15 Typical convergence of the optimization of A IV. In (**a**) the mean value of the output power of the μ selected individuals is plotted versus the number of generation. The corresponding decrease of the variance (as long as the success rate is <1/5) is shown in (**b**). Accordingly the graphs for a voltage optimization run are plotted in (**c**) and (**d**)

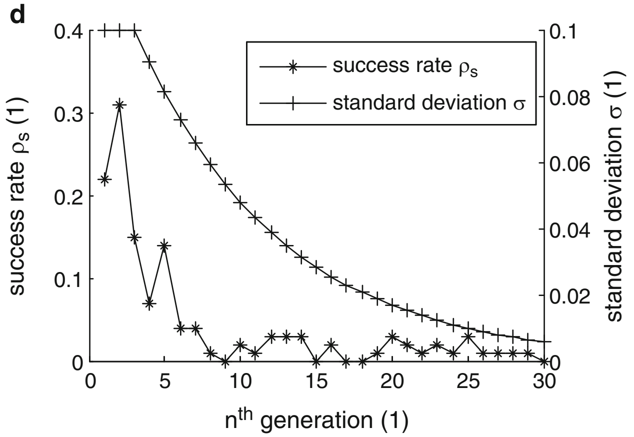

Fig. 4.15 (continued)

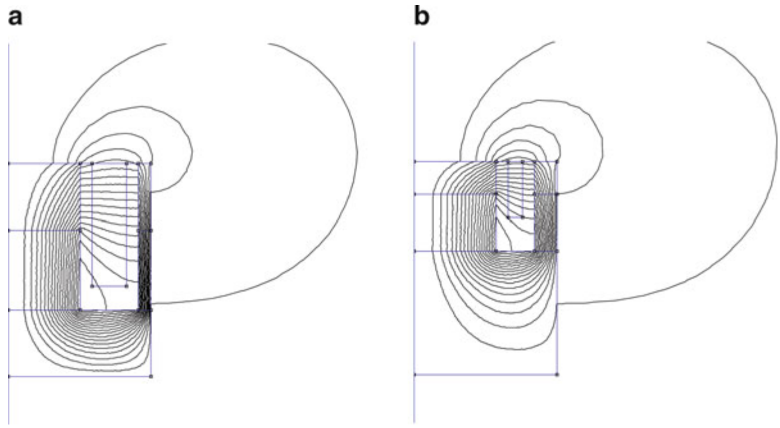

Fig. 4.16 (**a**) power optimized dimensions and (**b**) voltage optimized dimensions of A IV

radius $R_{i,mag}$ and the height of the ring magnet h_{mag}, the inner radius $R_{i,upp}$ and the height of the upper pole plate h_{upp} and the radius of the pole core R_{pc}. Figure 4.18a, b show the convergence of an output power ES optimization run. About 30 generations are necessary until the output power shows no significant increase and the stop criterion is fulfilled. The best individual was taken from generation 28. In this optimization run the success rate after the 3rd generation was smaller than 1/5 which causes the standard deviation to decrease continuously from the fourth generation on. The convergence of an output voltage optimization run is shown in Fig. 4.18c, d. The best individual was within the 25th generation. As for A IV the algorithm for output voltage optimization converges faster than for the output power optimization. A possible reason for that is that the voltage optimized coils are

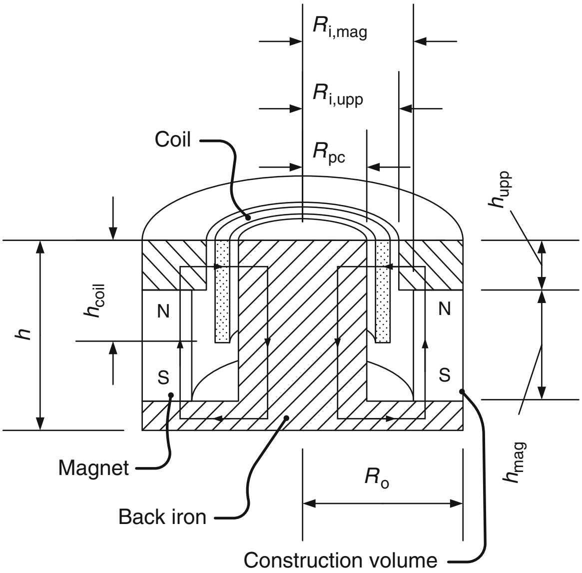

Fig. 4.17 Geometrical parameters of "Magnet in–line coil" architecture with back iron A V. The *closed loop* indicates the direction of magnetic flux

greater than the output power optimized coils which downsize the interval between the parameter bound.

The magnetic field pattern for output power and output voltage optimized dimensions of A V is shown in Fig. 4.19a, b. With these optimized dimensions a maximum output power of 6.72 mW can be generated at a voltage level of 1.99 V and a maximum output voltage of 3.49 V at a power level of 4.00 mW. Just as for A IV the coil volume of the output power optimized design (38 mm³) is almost five times smaller than the volume of the output voltage optimized design (179 mm³). Another characteristic as to that observed in A IV is that it is advantageous to set the inner radius of the upper pole plate equal to the inner radius of the magnet.

4.3 "Magnet Across Coil" Architectures

4.3.1 Architecture A VI

In architecture A VI two opposite polarized magnets move across a cylindrical coil. This is the first architecture with a cubic geometry. The geometrical parameters are shown in Fig. 4.20. As stated in the introduction the 1 cm³ construction volume (defined by the cuboid $a \cdot b \cdot h$) is 10·10·10 mm³. Because the magnetic circuit is not closed the magnetic field drops rapidly after the magnetic pole. Hence an elongated construction volume will be rather disadvantageous. By definition the border of the

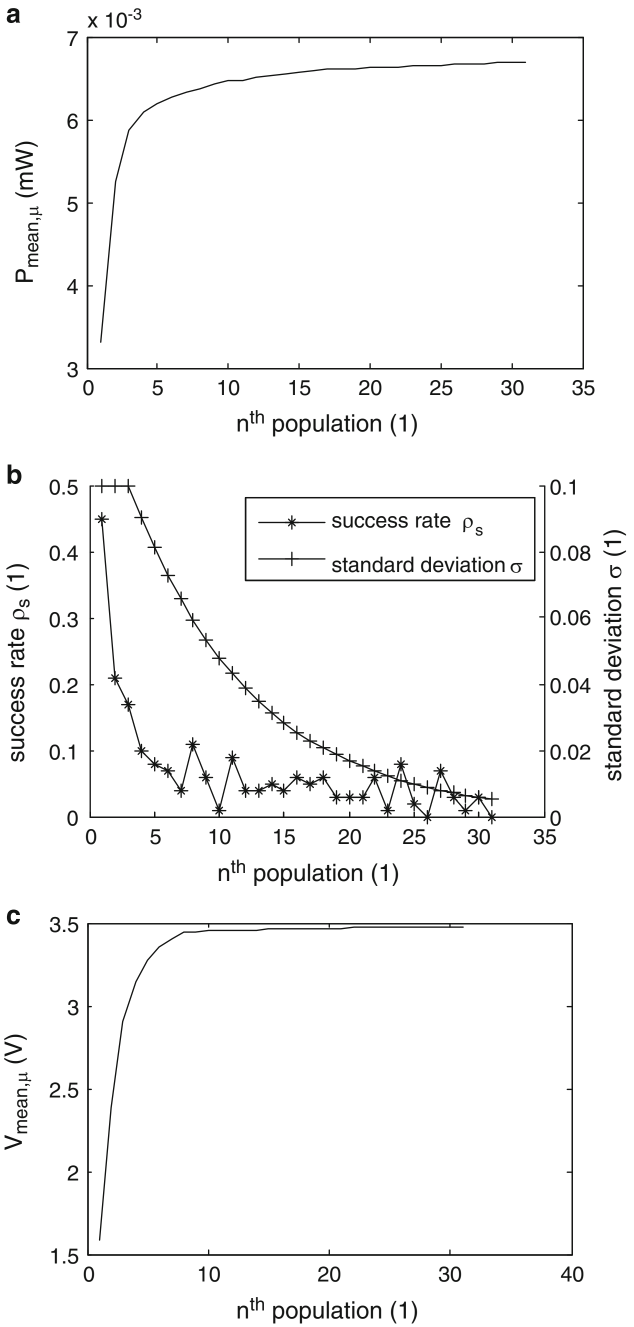

Fig. 4.18 Typical convergence of the optimization of A V. The mean value of the output power of the μ selected individuals is plotted in (**a**). The corresponding decrease of the variance (as long as the success rate is <1/5) is shown in (**b**). Accordingly the graphs for a voltage optimization run are plotted in (**c**) and (**d**)

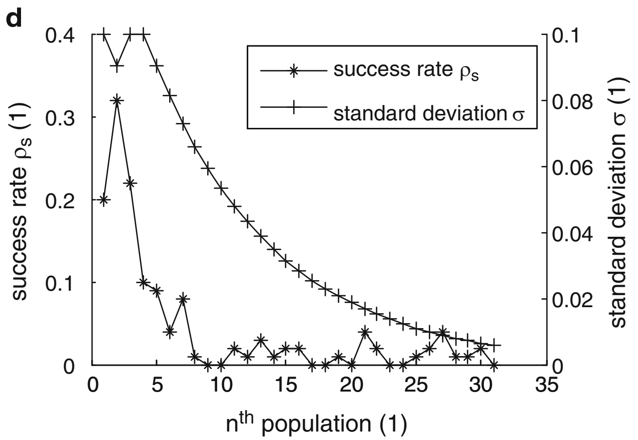

Fig. 4.18 (continued)

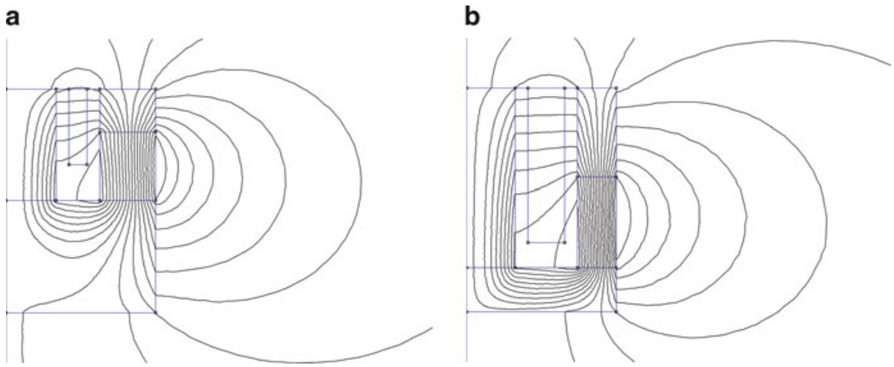

Fig. 4.19 (**a**) power optimized dimensions and (**b**) voltage optimized dimensions of A V

coil must not exceed the construction volume at the maximum inner displacement. On this note the outer radius of the coil R_o is given by:

$$R_o = \frac{b}{2} - z_{\max}. \tag{4.4}$$

(This definition of the outer radius is also valid for the architectures A VII and A VIII). Therewith the outer radius of the coil is fixed and two independent geometrical parameters remain, which need to be optimized. In the same manner as for the "Magnet in–line coil" architectures without back iron these are namely the inner radius and the height of the coil.

The results of the optimization are shown in Fig. 4.21. Because the mass of the magnet depends on the height of the coil but not on the inner radius of the coil the relative inner displacement amplitudes are almost horizontal isolines. However, at large inner radii and small coil heights the electromagnetic damping drops and

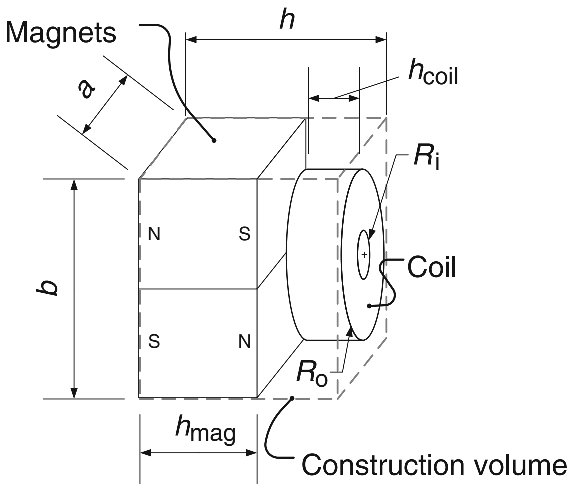

Fig. 4.20 Geometrical parameters of "Magnet across coil" architecture without back iron A VI

thus the inner displacement amplitude rises for mentioned reasons (refer to A II in Sect. 4.2.2). Another similarity to A II is that the maximum of the transduction factor and the optimum of the output voltage are located at the minimum inner radius of the coil (as in A II set to $R_{i,min} = 0.5$ mm). However in A VI this is also the case for the output power. As for the architectures A I–A III the maximum of the transduction factor is shifted to higher inner displacement amplitudes with respect to the optimum of the output voltage and the optimum of the output power is further shifted to higher oscillation amplitudes and smaller resistances with respect to the optimum of the output voltage. The highest possible output power is 3.76 mW at 1.58 V for a coil with 0.5 mm inner radius and 1.3 mm height (55 mm^3 coil volume). The optimal output voltage is obtained for a coil with minimal inner radius of 0.5 and 3.2 mm height (100 mm^3 coil volume). Therewith 1.96 V can be obtained at a power level of 2.26 mW. The optimal dimensions are shown in Fig. 4.22. The coil volume for voltage optimized dimensions is two times greater than the coil volume for power optimized dimensions. Consequently both the output power and the output voltage optimized dimensioning are more sensitive to the coil height than to the coil inner radius.

4.3.2 Architecture A VII

In contrast to the architecture A VI there are two opposite polarized magnets on both sides of the coil in architecture A VII. The geometrical parameters are shown in Fig. 4.23. Due to the field homogenization between the magnets (refer to Sect. 3.4) the aspect ratio of the 1 cm^3 construction volume applied in the optimization is rather elongated ($a = 8.7$ mm, $b = 8.7$ mm and $h = 13.21$ mm). Apart from this difference, the inner radius and the height of the coil are again the geometrical parameters which need to be optimized. The results of the optimization are shown in Fig. 4.24.

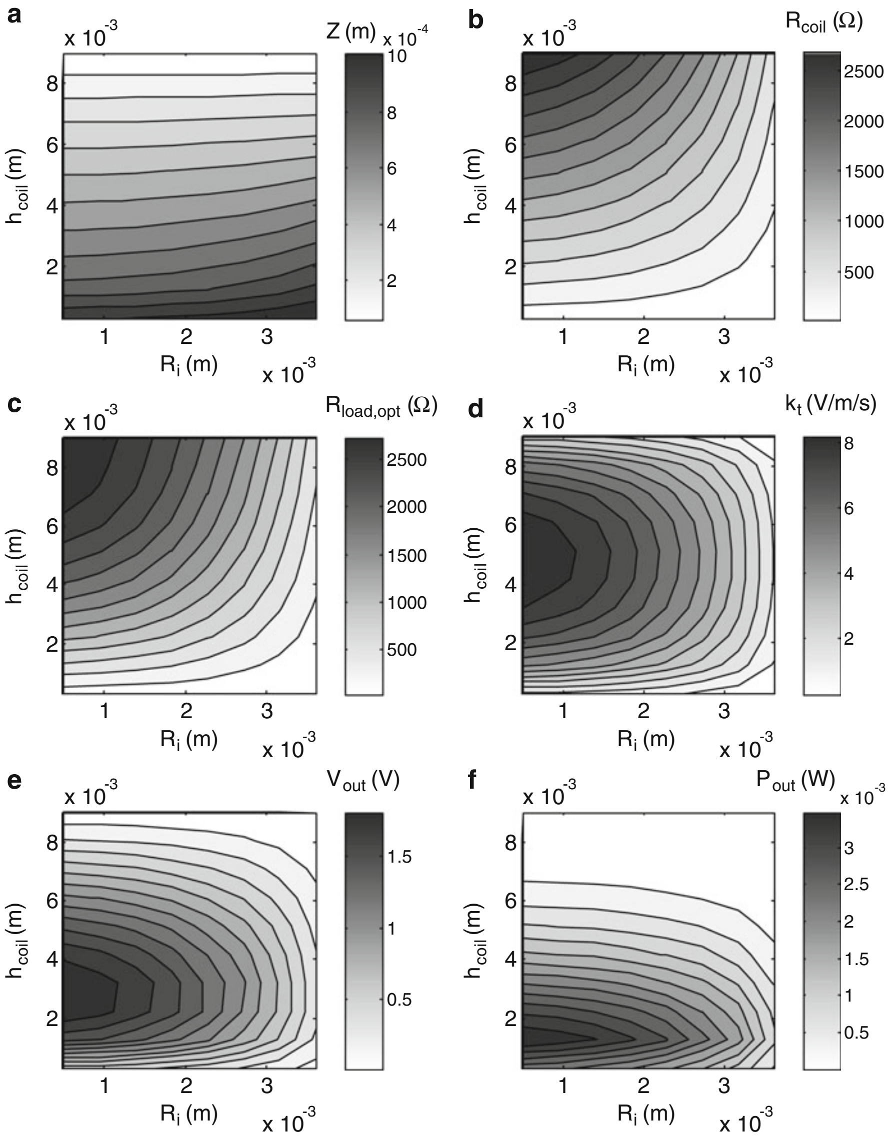

Fig. 4.21 Optimization result for A VI in a construction volume of 1 cm³. The figures show the resulting (**a**) inner displacement amplitude, (**b**) coil resistance, (**c**) optimal load resistance for different dimensions of the coil. There are definitely different optimal dimensions for maximizing (**d**) the magnetic flux gradient, (**e**) the output voltage and (**f**) the output power

Due to the similarity to A VI the results are also quite similar from the qualitative point of view. The highest possible output power is 5.56 mW at 2.17 V for a coil with the minimum inner radius of 0.5 and 1.54 mm height (53 mm³ coil volume).

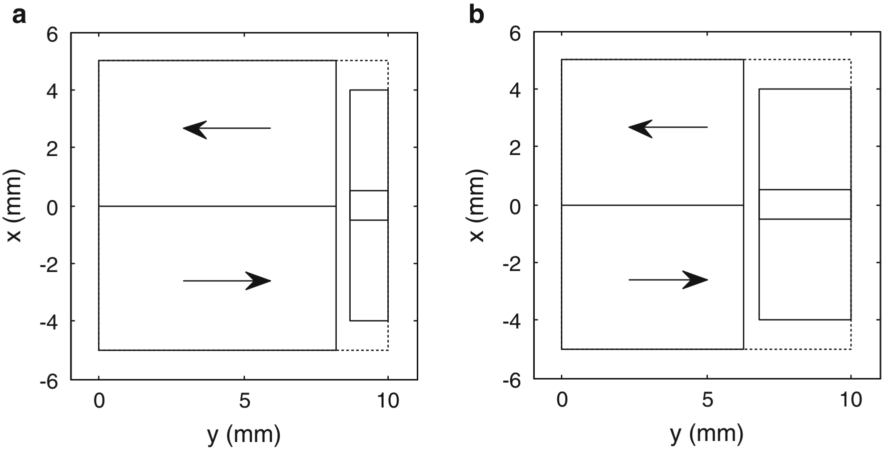

Fig. 4.22 Optimal dimensions for (**a**) output power and (**b**) output voltage generation with A VI. The *arrows* point from north to south pole

Fig. 4.23 Geometrical parameters of "Magnet across coil" architecture without back iron A VII

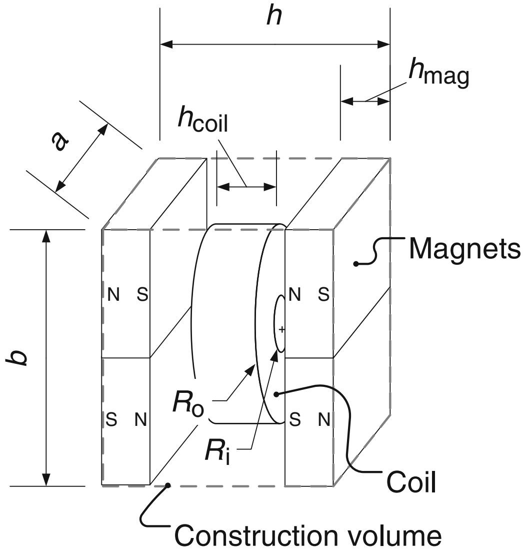

The optimal output voltage results with a minimal inner radius of 0.5 mm and a coil height of 2.79 mm (96 mm^3 coil volume). Therewith 2.51 V can be obtained at a power level of 4.25 mW. The optimal dimensions are shown in Fig. 4.25. The coil volume for voltage optimized dimensions is approximately two times greater than the coil volume for power optimized dimensions. It is apparent that in accordance to A VI both the output power and the output voltage optimized dimensioning are more sensitive to the coil height than to the coil inner radius.

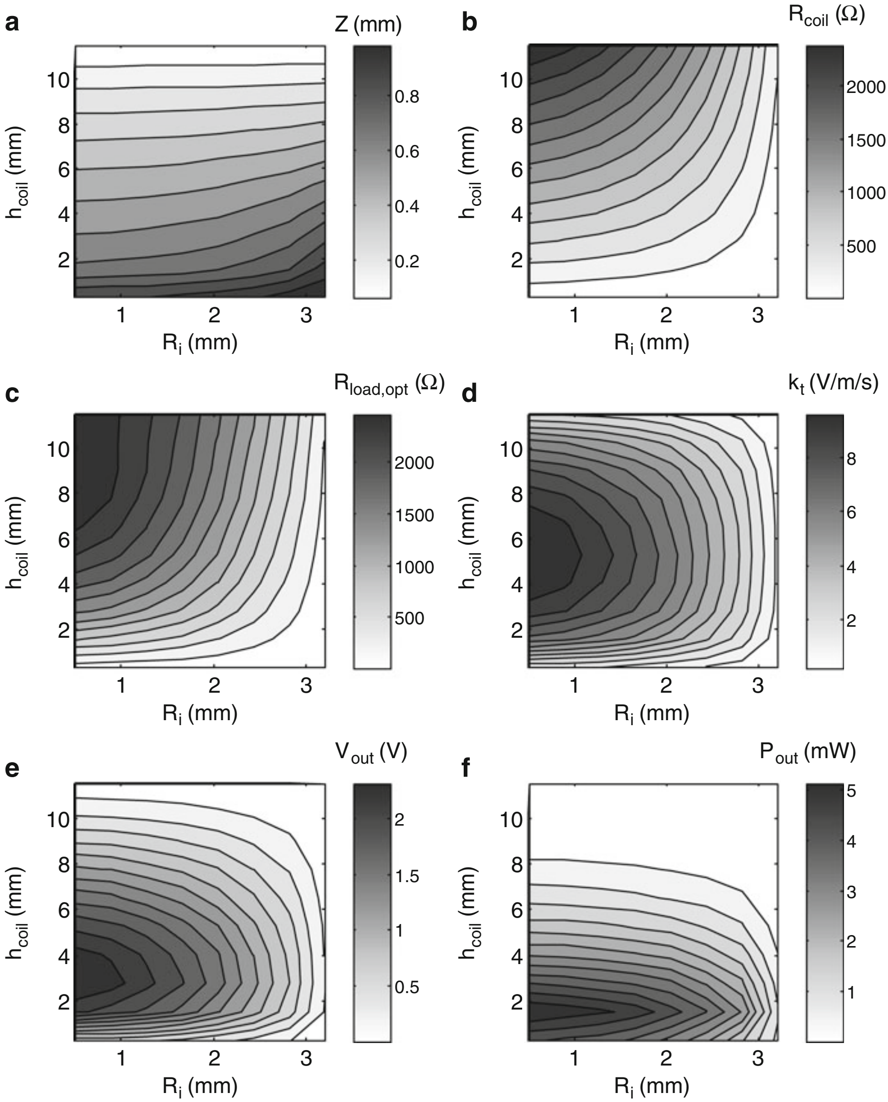

Fig. 4.24 Optimization result for A VII in a construction volume of 1 cm³. The figures shows the resulting (**a**) inner displacement amplitude, (**b**) coil resistance, (**c**) optimal load resistance for different dimensions of the coil. There are definitely different optimal dimensions for maximizing (**d**) the magnetic flux gradient, (**e**) the output voltage and (**f**) the output power

4.3.3 Architecture A VIII

In this architecture back iron is used to close the magnetic circuit partly. Apart from that the architecture is identical to A VII. The geometrical parameters are shown

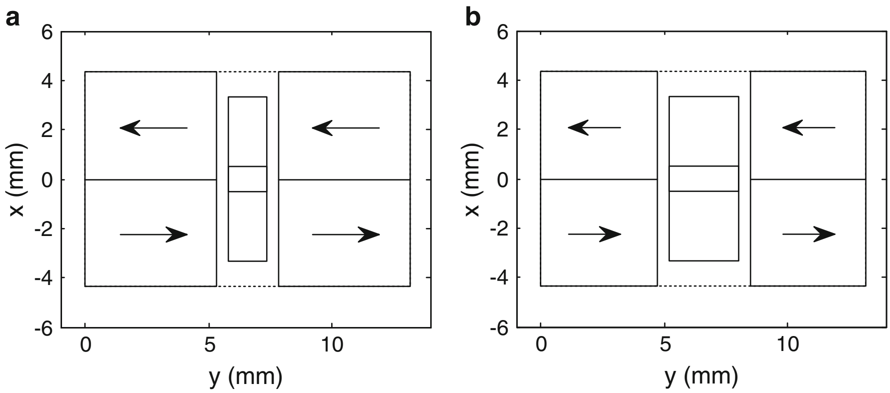

Fig. 4.25 Optimal dimensions for (**a**) output power and (**b**) output voltage generation with A VII. The *arrows* point from north to south pole

Fig. 4.26 Geometrical parameters of “Magnet across coil” architecture with back iron A VIII

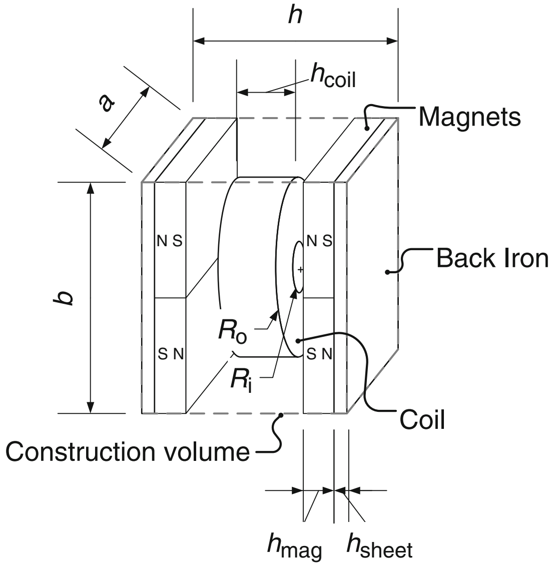

in Fig. 4.26. The height of the back iron sheet implicates a further geometrical parameter (h_{sheet}) which needs to be optimized. The results from the last “Magnet across coil” architectures show that the optimum of the output power and the optimum of the output voltage is obtained for a minimal inner radius of the coil. Moreover the output performance is quite insensitive against the inner radius of the coil. Consequently, it is expected that this is also true for A VIII. The inner radius of the coil has therefore been fixed to the minimum value of 0.5 mm. Therewith the remaining geometrical parameters to be optimized are the height of the magnet

h_{mag} and the height of the back iron sheet h_{sheet}. Because the height of the coil is a function of the height of the magnet and the back iron sheet:

$$h_{coil} = h - 2\left(h_{mag} - h_{sheet} - G\right), \tag{4.5}$$

it would also be possible to choose the height of the coil as a geometrical parameter. However, some interesting results can be shown when using the height of the magnet and the height of the back iron sheet as the geometrical parameters. The results of the optimization are shown in Fig. 4.27. Due to the different geometrical parameters with respect to the previous "Magnet across coil" architectures the diagrams look different.

The triangle shaped white area in the diagrams indicates the region that is not allowed because the sum of the two gaps, the back iron– magnet– and minimum coil height (set to 0.3 mm) are greater than the predefined construction volume length (13.21 mm). Apart from that the interpretation of the results is quite clear. The inner displacement (Fig. 4.27a) depends on the oscillating mass. Even though the density of the magnet and the back iron material are slightly different it does not matter whether the mass is produced by a thick magnet and a thin back iron sheet or vice versa. Hence the isolines of the inner displacement are just diagonal. Concerning the internal resistance it is clear that the thinner the sum of the magnet and the back iron sheet height the larger the height of the coil and consequently also the internal resistance. The same holds for the optimal load resistance. However for the magnetic flux gradient there is a maximum within the defined design domain. Again the maximum is shifted towards higher oscillation amplitudes concerning the output voltage and further shifted to higher oscillation amplitudes and smaller resistances concerning the output power. An interesting outcome of the optimization is that the dimensioning of A VIII is more sensitive to the sum of the magnet and the back iron sheet height than to the height of each single parameter. That means that it does not matter whether the oscillating mass is provided by a large magnet height and a small back iron sheet height or vice versa. A low–cost implementation of A VIII would therefore use a small magnet and large back iron sheet without having a disadvantage in the output performance. With the optimal magnet height of 3.30 mm and back iron sheet height of 2.29 mm an output power of 5.83 mW can be generated at a voltage level of 1.72 V. The optimal output voltage dimensions are 2.97 mm magnet height and 1.67 mm sheet height. With these dimensions 2.47 V can be generated at a power level of 4.09 mW. The optimal dimensions are shown in Fig. 4.28.

4.4 Conclusion and Comparison of the Coupling Architectures

In the previous subsections the results of the output power and output voltage optimization of eight different electromagnetic coupling architectures have been presented. In order to assess the most efficient coupling architectures this subsection

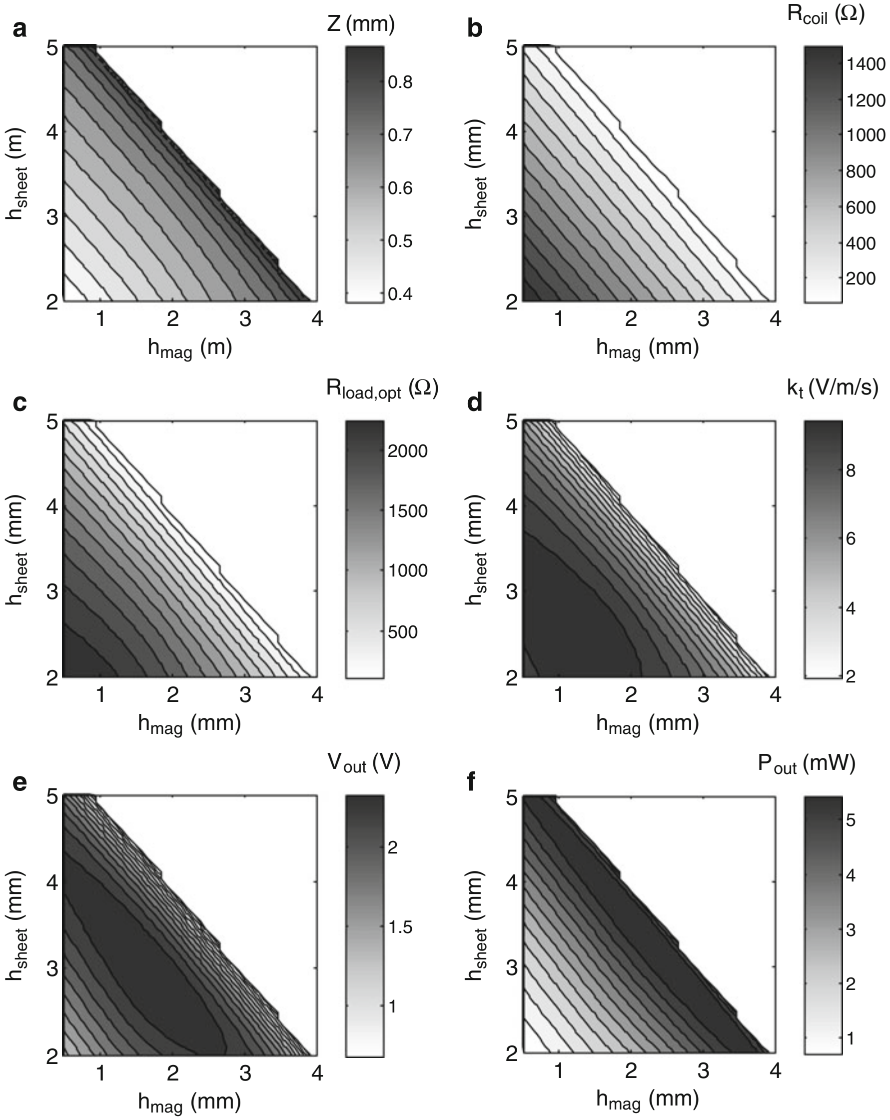

Fig. 4.27 Optimization result for A VII in a construction volume of 1 cm³. The figures shows the resulting (**a**) inner displacement amplitude, (**b**) coil resistance, (**c**) optimal load resistance for different dimensions of the magnet and back iron sheet. There are definitely different optimal dimensions for maximizing (**d**) the magnetic flux gradient, (**e**) the output voltage and (**f**) the output power

is concerned with the comparison of the architectures performance limit. As a basis for this comparison the same boundary conditions (including the parasitic damping) have been applied in the optimization calculations. Nevertheless the

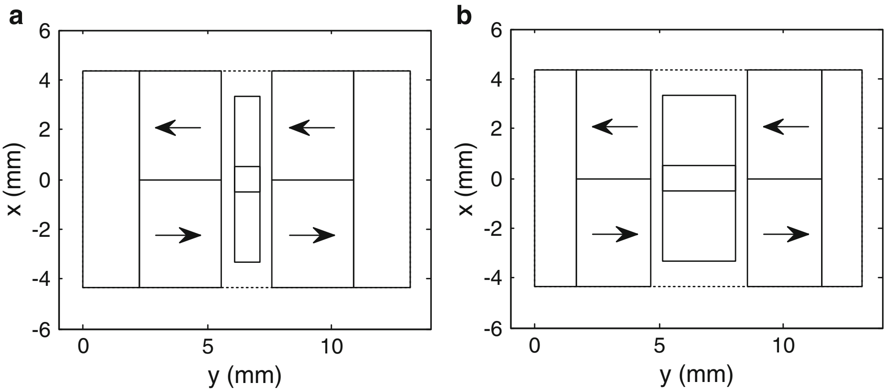

Fig. 4.28 Optimal dimensions for (**a**) output power and (**b**) output voltage generation with A VIII. The *arrows* point from north to south pole

parasitic damping is assumed to be dominated by the aerodynamic resistance which depends on the reference area and the drag coefficient. However these values depend on the design of the architecture. In order to investigate the variation of the performance limits with respect to the parasitic damping the optimization calculations have been repeated with $\pm 10\%$ of the parasitic damping coefficient. In the following comparison graphs these results are included as error bars.

4.4.1 Output Power Generation Capability

So far the dimensions of the architecture specific geometrical parameters (magnet, coil and back iron components) have been optimized. A basic outcome from the optimization procedure is that for each architecture there exists a different set of optimal geometrical parameters for maximum output power and maximum output voltage performance. Any other than these optimal dimensions will decrease the output performance. Fig. 4.29 shows a comparison of the architecture dependent maximum output power and the corresponding output voltage (dashed lines indicate the mean values of all architectures). The result shows that with respect to the overall boundary conditions architectures A V is definitely capable of generating the highest output power in a construction volume of 1 cm^3. With almost the same output power architecture A VIII and A IV perform second best. Note that these best three architectures are the architectures with back iron. From there it seems that back iron has a general advantage for output power generation even though there is less space for the magnetic material. Although the loudspeaker based architectures A IV and A V are rather similar there is a moderate difference of 15% in the output power performance. The fourth best architecture with respect to the output power is A VII. At the same time this is the best architecture without back iron. The

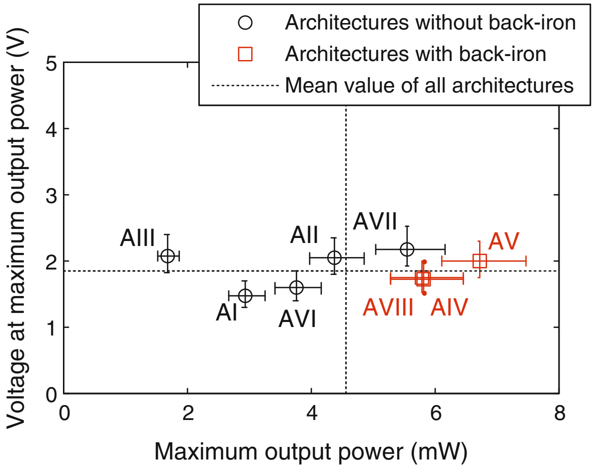

Fig. 4.29 Comparison of the maximum output power obtained with the optimal output power dimensions together with the corresponding voltage at the optimal output power points. The *dashed curve* indicates the mean value of all architectures. The *errorbars* indicate a variance of ±10% of the parasitic damping

remaining architectures are below the mean value of all architectures. The lowest output power is predicted with architecture A III. Note that there is a factor of 4 between the highest and the lowest output power. This emphasizes the fact, that beyond the optimization of the geometrical parameters it is of great importance to choose the right architecture for the application. The corresponding output voltage level at the maximum output power points can be used for further evaluation (primarily of the best architectures). In detail that means that an architecture with low output power performance does not become really better if the corresponding output voltage level is high but an architecture with high output power performance becomes even better if the output voltage level is also high. A prime example is the comparison of A VII and A VIII. With respect to the output power A VIII is only slightly better (5%). However the output voltage at optimal power point of A VII is 25% higher than in A VIII. In application this may be a reason to prefer A VII. There is no general advantage of the “Magnet in–line coil” or the “Magnet across coil” architecture class. In both classes there are architectures which are within the best.

4.4.2 Output Voltage Generation Capability

In the same way as for the output power Fig. 4.30 shows a comparison of the architectures maximum output voltage. It is architecture A II which is capable of generating the highest output voltage followed from the two loudspeaker based architectures A V and A IV. The “magnet across coil” architectures perform all below the mean value of all architectures. The “Magnet in–line coil” architectures seem to have a general advantage for output voltage generation (except architecture A I). The difference between the lowest and the highest values is not that large as

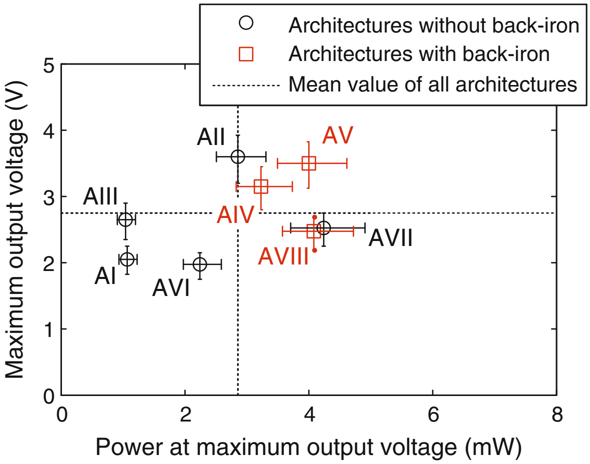

Fig. 4.30 Comparison of the architectures maximum output voltage obtained with the optimal output voltage dimensions together with the corresponding power at the optimal output voltage points. The *dashed curve* indicates the mean value of all architectures. The *errorbars* indicate a variance of ±10% of the parasitic damping

for the output power optimization but is still a factor of 1.8. Accordingly the power level at the optimal voltage points can be used for further evaluation. Even though A II is capable of generating a slightly higher output voltage than A V the output power level of A V is significantly higher (40%). Hence A V should be preferred whenever possible. Another interesting fact is that A III has indeed a moderate voltage generation capability but the corresponding output power is quite low.